THE JOURNAL OF BIOLOGICAL CHEMISTRY VOL. 283, NO. 45, pp. 30933–30941, November 7, 2008

Agonist-selective, Receptor-specific Interaction of Human P_{2Y} Receptors with β-Arrestin-1 and -2*Ⓢ

Received for publication, February 22, 2008, and in revised form, July 25, 2008 Published, JBC Papers in Press, August 14, 2008, DOI 10.1074/jbc.M801472200

Carsten Hoffmann[1], **Nicole Ziegler, Susanne Reiner, Cornelius Krasel**[2], **and Martin J. Lohse**
From the Institute for Pharmacology and Toxicology, Versbacher Strasse 9, D-97078 Wuerzburg, Germany

Interaction of G-protein-coupled receptors with β-arrestins is an important step in receptor desensitization and in triggering "alternative" signals. By means of confocal microscopy and fluorescence resonance energy transfer, we have investigated the internalization of the human P2Y receptors 1, 2, 4, 6, 11, and 12 and their interaction with β-arrestin-1 and -2. Co-transfection of each individual P2Y receptor with β-arrestin-1-GFP or β-arrestin-2-YFP into HEK-293 cells and stimulation with the corresponding agonists resulted in a receptor-specific interaction pattern. The $P2Y_1$ receptor stimulated with ADP strongly translocated β-arrestin-2-YFP, whereas only a slight translocation was observed for β-arrestin-1-GFP. The $P2Y_4$ receptor exhibited equally strong translocation for β-arrestin-1-GFP and β-arrestin-2-YFP when stimulated with UTP. The $P2Y_6$, $P2Y_{11}$, and $P2Y_{12}$ receptor internalized only when GRK2 was additionally co-transfected, but β-arrestin translocation was only visible for the $P2Y_6$ and $P2Y_{11}$ receptor. The $P2Y_2$ receptor showed a β-arrestin translocation pattern that was dependent on the agonist used for stimulation. UTP translocated β-arrestin-1-GFP and β-arrestin-2-YFP equally well, whereas ATP translocated β-arrestin-1-GFP to a much lower extent than β-arrestin-2-YFP. The same agonist-dependent pattern was seen in fluorescence resonance energy transfer experiments between the fluorescently labeled $P2Y_2$ receptor and β-arrestins. Thus, the $P2Y_2$ receptor would be classified as a class A receptor when stimulated with ATP or as a class B receptor when stimulated with UTP. The ligand-specific recruitment of β-arrestins by ATP and UTP stimulation of $P2Y_2$ receptors was further found to result in differential stimulation of ERK phosphorylation. This suggests that the two different agonists induce distinct active states of this receptor that show differential interactions with β-arrestins.

G-protein-coupled receptors (GPCRs)[3] can be stimulated by diverse signals such as light, smell and taste, small molecules, peptides, and proteins. Their stimulation is transduced across the plasma membrane by conformational changes and leads to the activation of heterotrimeric G-proteins (1). This receptor signal is turned off by desensitization and internalization of GPCRs. These processes are triggered through receptor phosphorylation either by second messenger-activated kinases or by G-protein-coupled receptor kinases (GRKs) (2). Receptor phosphorylation by GRKs leads to binding of β-arrestins to the receptors causing uncoupling from their G-proteins (3). In recent years it has become evident that the recruitment of β-arrestins also leads to the activation of alternative signaling pathways, including MAPK signaling (4).

Differential affinities of GPCRs for β-arrestin-1 or -2 were first described by Oakley *et al.* (5) employing fluorescently tagged β-arrestins and the use of confocal microscopy. This work classified GPCRs as class A if the receptor bound β-arrestin-2 with higher affinity than β-arrestin-1, or class B receptors if β-arrestin-1 and -2 were bound with similar affinities. Although class A receptors are prone to rapid recycling to the plasma membrane, class B receptors often undergo endosomal degradation or slow recycling to the plasma membrane (6). Because of this behavior and because β-arrestin-1 or -2 has been suggested to have differential effects in downstream signaling (6), it has become important to know the potential β-arrestin binding profile of individual members of the GPCR family.

Purine receptors are pharmacological targets in processes as diverse as platelet aggregation and treatment of cystic fibrosis (7, 8). The P2Y receptor family is composed of currently eight members that are all GPCRs, termed $P2Y_1$, $P2Y_2$, $P2Y_4$, $P2Y_6$, $P2Y_{11}$, $P2Y_{12}$, $P2Y_{13}$, and $P2Y_{14}$ (9). The first five members compose a subgroup that principally uses G_q/G_{11} to activate the phospholipase-β/1,4,5-myoinositol trisphosphate pathway, whereas the other three represent a second subgroup and almost exclusively couple to the $G_{i/o}$ family of G-proteins (8). Although in the recent past a lot has been learned about signaling and tissue distribution of P2Y family members (10), much less is known about their desensitization or internalization (11–13).

Therefore, we studied the internalization and β-arrestin translocation behavior of members of the P2Y receptor family.

* This work was supported by the Deutsche Forschungsgemeinschaft Grant "Sonderforschungsbereich" SFB487 "Regulatory Membrane Proteins," by the Fonds der Chemischen Industrie, and by the Ernst-Jung Award for Medicine. The costs of publication of this article were defrayed in part by the payment of page charges. This article must therefore be hereby marked "*advertisement*" in accordance with 18 U.S.C. Section 1734 solely to indicate this fact.

Ⓢ The on-line version of this article (available at http://www.jbc.org) contains supplemental Figs. S1–S5 and Movies 1–9.

[1] To whom correspondence should be addressed. E-mail: c.Hoffmann@toxi.uni-wuerzburg.de.

[2] Present address: University of Reading, School of Pharmacy, Whiteknights, P. O. Box 228, Reading, Berkshire RG6 6AJ, United Kingdom.

[3] The abbreviations used are: GPCR, G-protein-coupled receptor; FRET, fluorescence resonance energy transfer; GFP, green fluorescent protein; GRK, G-protein-coupled receptor kinase; MRS2179, 2′-deoxy-*N*[6]-methyladenosine 3′,5′-bisphosphate; CFP, cyan fluorescent protein; YFP, yellow fluorescent protein; MAPK, mitogen-activated protein kinase; ERK, extracellular signal-regulated kinase.

All receptors were individually fused at their C termini with various color variants of the green fluorescent protein (GFP), and their internalization was monitored by confocal microscopy. For all receptors, we investigated the internalization and β-arrestin translocation behavior in an identical cellular background, thus allowing a comparison of individual receptor subtypes and a classification into classes A and B with respect to their β-arrestin interaction profiles.

EXPERIMENTAL PROCEDURES

Materials—ADP, ATP, UDP, UTP, 2-methylthio-ADP hexokinase, poly-D-lysine, and glucose were purchased from Sigma. MRS2179 was purchased from Tocris (Northpoint, UK). Cell culture reagents were supplied from PAN-Biotech GmbH (Aidenbach, Germany). Effectene was purchased from Qiagen (Hilden, Germany). Lipofectamine-2000 was purchased from Invitrogen. 1321N1 astrocytoma cells were purchased form ECACC (Porton Down, Whiteshire, UK). The cDNA for the human $P2Y_1$ receptor has been described previously (14). cDNAs for human $P2Y_2$, $P2Y_4$, $P2Y_6$, $P2Y_{11}$, and $P2Y_{12}$ receptors were purchased from the on-line cDNA Resource Center (University of Missouri-Rolla). All PCR primers were synthesized by MWG-Biotec GmbH (Ebersberg, Germany). Sequencing reactions were done by Eurofins Medigenomix GmbH (Martinsried, Germany). Rabbit polyclonal p44/42 MAPK antibody and rabbit polyclonal anti-phospho-p44/42 MAPK (Thr-202/Tyr-204) antibody were purchased from Cell Signaling. Horseradish peroxidase-conjugated polyclonal goat anti-rabbit antibody was purchased from Dianova. All other chemicals were purchased from commercial suppliers at the highest purity grade available.

Construction of P2Y Receptors Tagged with Fluorescent Proteins (XFP)—Each of the six P2Y receptors was fused to the enhanced variants of cyan (CFP) or yellow (YFP) fluorescent protein (Clontech) by the standard PCR extension overlap technique (15). In each case the C-terminal stop codon of the receptor and the initial codon for methionine of the fluorescent protein were deleted. Hence, no linker sequence exists between the receptor and the fluorescent protein. All resulting constructs were cloned into pcDNA3 (Invitrogen) and confirmed by sequencing.

β-Arrestin Constructs—Throughout all confocal microscopic analyses described in this study, we used bovine β-arrestin-1 fused C-terminally to enhanced GFP and bovine β-arrestin-2 fused C-terminally to enhanced YFP as described previously (16). GFP and YFP were used to distinguish data from both subtypes easily by color. The selection of the fluorescent protein had no influence on the translocation behavior (data not shown). For measurements of FRET, we used bovine β-arrestin-1 or -2 fused to CFP or the cerulean variant (17) generated following procedures as described previously (16).

Cell Culture—HEK-293 cells, COS-1 cells, and 1321N1 astrocytoma cells were maintained in Dulbecco's modified Eagle's medium with 4.5 g/liter glucose, 10% fetal calf serum, 100 units/ml penicillin G, and 100 μg/ml streptomycin sulfate at 37 °C, 7% CO_2. All cells were routinely passaged every 2–3 days. Culture medium for cells stably expressing the $P2Y_2$-YFP receptor was additionally supplemented with 200 μg/ml G-418.

Characterization of Receptor Constructs—The P2Y receptor-XFP fusion constructs were functionally tested in cell types lacking the respective endogenous receptor measuring inositol phosphate production. For $P2Y_1$ and $P2Y_6$ receptor constructs, inositol phosphate production was determined in COS-1 cells. COS-1 cells were transfected using the DEAE-dextran method and were assayed as described previously (14, 18). To minimize contaminations of UTP, UDP was preincubated with hexokinase and glucose for 1 h; this method quantitatively converts contaminating UTP into UDP (19). The $P2Y_2$, $P2Y_4$, and $P2Y_{11}$ receptor were determined in 1321N1 cells as described (19). 1321N1 cells were transfected using Lipofectamine. The functionality of the $P2Y_{12}$ receptor construct has been described previously (20).

Transfection of HEK-293 Cells for Microscopic Analysis—Individual 24-mm glass coverslips were placed in 6-well plates and coated for 30–60 min using 300 μl of poly-D-lysine (1 mg/ml). Poly-D-lysine was aspirated, and the glass coverslips were washed once with sterile phosphate-buffered saline without Ca^{2+}. HEK-293 cells were seeded onto these coverslips to result in ~50% confluence. After attachment of the cells (4–6 h), cells were transfected using Effectene according to the manufacturer's instructions. The following amounts of DNA were used per well: 300 ng for receptors, 200 ng for β-arrestins, 300 ng for dynamin Ia or DynK44A mutant (21), and 200 ng for GRK2. All constructs were in pcDNA3, except dynamin and DynK44, which were in pCMV5 vector; the amount of DNA was adjusted using empty pcDNA3 vector. Medium was exchanged 12–16 h later, and cells were analyzed 48 h after transfection.

Confocal Microscopy—All confocal microscopy experiments were performed on a Leica TCS SP2 system. Coverslips with transfected HEK-293 cells were mounted using an "Attofluor" holder (Molecular Probes, Leiden, The Netherlands). Images were taken with a 63× objective. CFP was excited with a 430 nm diode laser using a DCLP455 dichroic mirror. Fluorescence intensities were recorded from 470 to 550 nm. GFP was excited using the 488 nm line of an argon laser and a DCLP500 dichroic mirror. Fluorescence intensities were recorded from 500 to 550 nm. YFP was excited with the 514 nm line of the argon laser and a dual beam splitter 458/514 nm. Fluorescence intensities were recorded from 525 to 600 nm. Settings for recording images were kept constant: 512 × 512 pixel format, line average 4, 400 Hz, resulting in an image acquisition time of 7 s. Time series were recorded using the standard Leica software package (version 2.5). Pictures were taken at 1-min intervals.

Quantification of β-arrestin translocation was done with the Leica software package (version 2.5.). Regions of interest were defined in the cytosol and quantified over the time recorded. Care was taken that slight movements of the cells did not result in misplacement of the defined region of interest either onto the membrane or into the nuclear region. To correct for possible photobleaching, control regions were defined that included whole cells and were used to correct the images in the cytosolic regions of interest. The resulting fluorescence intensity values were then normalized to the initial value and plotted against time to quantify β-arrestin translocation from the cytosol.

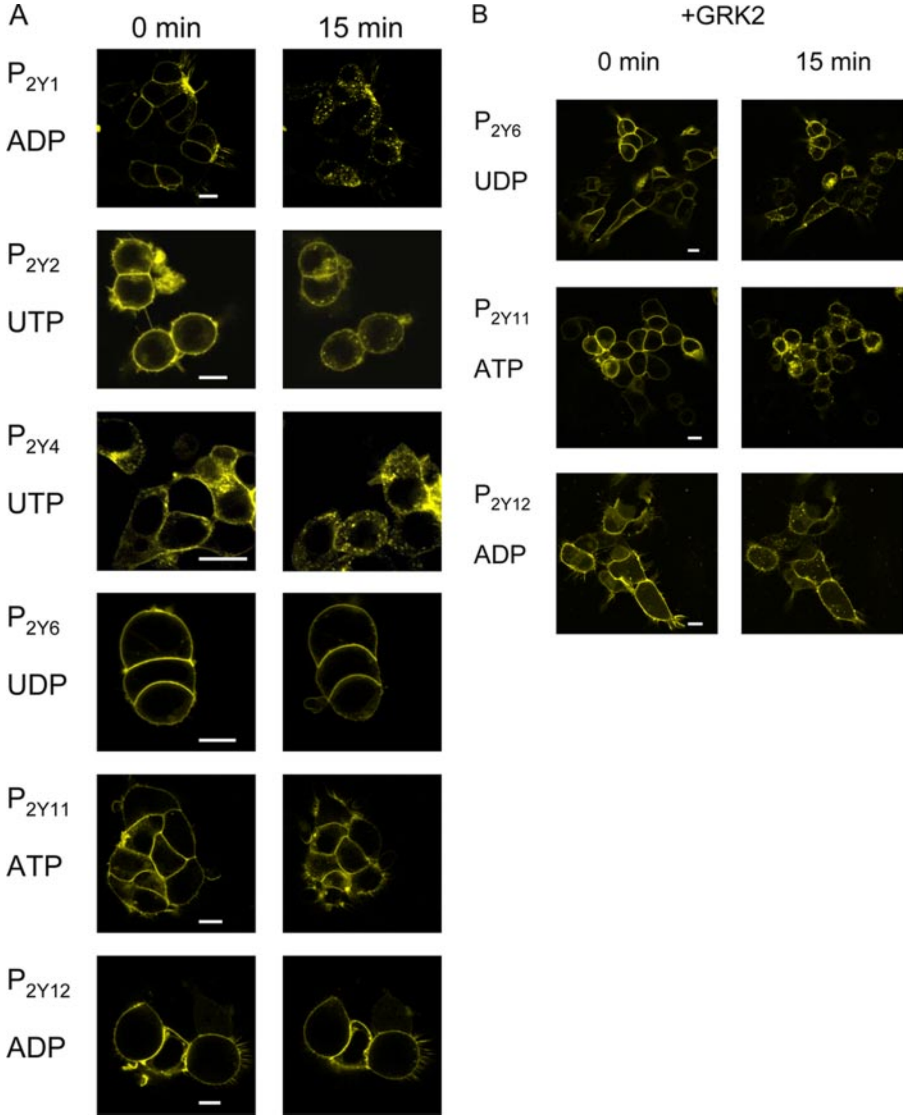

FIGURE 1. **Agonist-induced internalization of YFP-tagged $P2Y_{1,2,4,6,11,12}$ receptors in HEK-293 cells.** Cells were transfected with fluorescently tagged P2Y receptor constructs and studied for receptor internalization. *A, left column* represents cells prior to stimulation with the indicated agonist. The *right column* shows the same cells 15 min after exposure to the indicated agonist. A punctate pattern occurred for the $P2Y_1$, $P2Y_2$, and $P2Y_4$ receptor, whereas no punctate pattern was observed for the $P2Y_6$, $P2Y_{11}$, and $P2Y_{12}$ receptor tagged with YFP. All agonist concentrations were 100 μM final. Data are representative examples of at least three individual experiments. The experiments are added as supplemental movies 1–6. *B,* cells were co-transfected with GRK2 and $P2Y_6$, $P2Y_{11}$, or $P2Y_{12}$ receptor tagged with YFP and studied for receptor internalization. The *left column* represents cells prior to stimulation with the indicated agonist. The *right column* shows the same cells 15 min after exposure to the indicated agonist. Under these conditions a punctate pattern did occur for the $P2Y_6$, $P2Y_{11}$, and $P2Y_{12}$ receptor tagged with YFP. All agonist concentrations were 100 μM final. Data are representative examples of at least three individual experiments. The experiments are added as supplemental movies 7–9. *White scale bars* represent 10 μm.

Movies of the individual images were produced using ImageJ software (NIH Image software). Solely for display reasons, but not for quantitative analyses, individual images were corrected for auto-contrast using Photoshop software version 6.0.

FRET Measurements—FRET was recorded between P2Y receptors tagged with YFP and bovine β-arrestin-1 tagged with cerulean or β-arrestin-2 tagged with CFP, respectively. The measurements were performed as described previously (16). Cells transfected as described above were washed with Hanks' balanced salt solution and maintained in buffer A (140 mM NaCl, 5 mM KCl, 2 mM $CaCl_2$, 1 mM $MgCl_2$, 10 mM Hepes, pH 7.3) at room temperature. Coverslips were mounted on an Attofluor holder and placed on a Zeiss inverted microscope (Axiovert135) equipped with an oil immersion 63× objective and a dual emission photometric system (Till Photonics). Samples were excited with light from a polychrome IV (Till Photonics). To minimize photobleaching, the illumination time was set to 10–40 ms, applied with a frequency of 10 Hz. The fluorescence signal was recorded from a single whole cell. FRET was monitored from the emission ratio of YFP to CFP, F_{535}/F_{480} (emission intensities at 535 ± 15 and 480 ± 20 nm, beam splitter DCLP 505 nm), upon excitation at 436 ± 10 nm (beam splitter DCLP 460 nm). The YFP emission upon excitation at 480 nm was recorded at the beginning of each experiment to subtract direct excitation of YFP (YFP emission at 436 nm excitation/YFP emission at 480 nm excitation was 0.065). The emission ratio was corrected by the spillover of CFP into the 535 nm channel (spillover of YFP into the 480 nm channel was negligible) to give a corrected ratio F^*_{535}/F^*_{480}. To determine agonist-induced changes in FRET, cells were continuously superfused with buffer A, and agonist was applied using a computer-assisted solenoid valve controlled rapid superfusion device ALA-VM8 (ALA Scientific Instruments; solution exchange 5–10 ms). Signals detected by avalanche photodiodes were digitized using an AD converter (Digidata1322A, Axon Instruments) and stored using Clampex 8.1 software (Axon Instruments).

Detection of ERK1/2 Phosphorylation—ERK1/2 phosphorylation was assessed in serum-starved (0.5% for 24 h) HEK-293 cells stably expressing the $P2Y_2$-YFP receptor at 80% confluence. 100 μM UTP or ATP (final concentration) was added for the indicated times, and ERK1/2 phosphorylation was assessed by Western blotting with phosphor-ERK-specific antibodies (rabbit polyclonal anti-phospho-p44/42 MAPK (Thr-202/Tyr-204) antibody, Cell Signaling). Total ERK was quantified as a reference using a rabbit polyclonal p44/42 MAPK antibody (Cell Signaling). Quantification was done by chemiluminescence using a horseradish peroxidase-conjugated polyclonal goat anti-rabbit antibody (Dianova) and a chemiluminescence reader (FujiFilm LAS-1000).

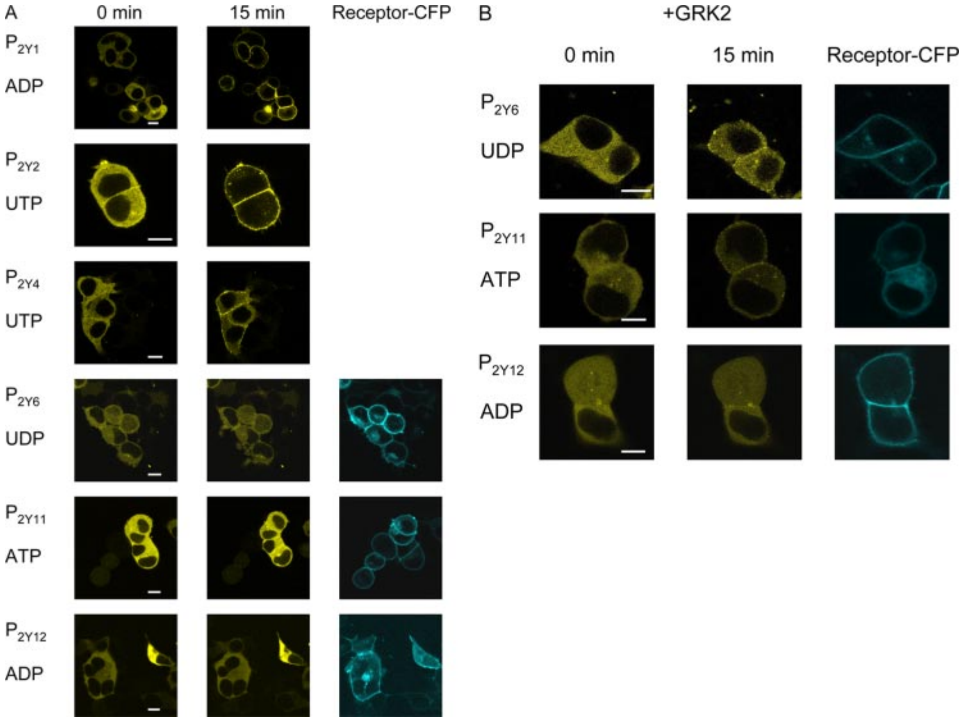

FIGURE 2. **β-Arrestin-2 translocation induced by stimulation of $P2Y_{1,2,4,6,11,12}$ receptor.** HEK-293 cells were co-transfected with the indicated P2Y receptor and β-arrestin-2-YFP construct. *A, left column* represents cells prior to stimulation with the indicated agonist. The *middle column* shows the same cells 15 min after exposure to the indicated agonist. A clear β-arrestin-2 translocation was observed for the $P2Y_1$, $P2Y_2$, and $P2Y_4$ receptor, whereas no β-arrestin-2 translocation was observed for the $P2Y_6$, $P2Y_{11}$, and $P2Y_{12}$ receptor. The *right column* shows localization of the CFP-tagged receptor construct to demonstrate co-transfection of the cells that were studied. All agonist concentrations were 100 μM final. Data are representative examples of at least three individual experiments. *B,* cells were co-transfected with GRK2, β-arrestin-2-YFP, and $P2Y_6$, $P2Y_{11}$, or $P2Y_{12}$ receptor tagged with CFP and studied for receptor internalization. The *left column* represents cells prior to stimulation with the indicated agonist. The *middle column* shows the same cells 15 min after exposure to the indicated agonist. A clear β-arrestin-2 translocation was observed for the $P2Y_6$ and $P2Y_{11}$ receptor, whereas no β-arrestin-2 translocation was seen for the $P2Y_{12}$ receptor. The *right column* shows localization of the CFP-tagged receptor construct to demonstrate co-transfection of the cells that were studied. All agonist concentrations were 100 μM final. Data are representative examples of at least three individual experiments. *White scale bars* represent 10 μm.

Receptor internalization was then studied by confocal microscopy of the YFP-tagged receptors transfected into HEK-293 cells. Pictures were taken prior to agonist stimulation and at 1-min intervals after addition of the respective specific agonist (100 μM final concentration). Fig. 1*A* shows the results for all P2Y receptor subtypes tested. Prior to agonist stimulation, clear membrane localization was observed for all receptor subtypes. Upon stimulation with the appropriate agonists the $P2Y_1$, $P2Y_2$, and $P2Y_4$ receptors rapidly internalized (supplemental movies 1–3), but no internalization was observed for the $P2Y_6$, $P2Y_{11}$, and $P2Y_{12}$ receptors (supplemental movies 4–6). However, the latter three receptors all internalized when G-protein-coupled receptor kinase 2 (GRK2) was co-transfected, as seen by the appearance of a distinct punctate pattern (Fig. 1*B*, *right* and supplemental movie 7–9). The membrane localization in the absence of agonist was unaffected by GRK2 (Fig. 1*B*, *left*). Specificity of the internalization was shown by the selectivity for the respective agonists. For example, we found internalization of the $P2Y_4$ receptor in response to UTP (Fig. 1*A*), but not to ATP (not shown), which is an antagonist at this receptor (23, 24).

RESULTS

β-Arrestin Translocation in Control HEK-293 Cells—HEK-293 cells have been described to express endogenously various P2Y receptors subtypes (10, 22). Therefore, we first investigated whether these receptors would interfere with our study by inducing β-arrestin translocation to the cell surface. To do so, we investigated HEK-293 cells transfected with β-arrestin-1-GFP or β-arrestin-2-YFP by confocal microscopy. None of the four endogenous purine receptor agonists ADP, ATP, UDP, and UTP (100 μM) caused any change in the cytosolic localization of either β-arrestin (supplemental Fig. 1). From these experiments we conclude that endogenous purine receptors did not interfere with the following experiments.

Receptor Internalization upon Agonist Stimulation—To study the internalization of P2Y receptors, we tagged each receptor at the C terminus with YFP. Similarly to the GFP-tagged $P2Y_{12}$ receptor (20), all receptors were functional with respect to downstream inositol phosphate signaling. In each case, the maximal responses to agonist stimulation were similar, and the EC_{50} values for agonist-induced inositol phosphate production were shifted less than 3-fold to higher agonist concentrations when compared with the corresponding wild-type receptors (data not shown).

β-Arrestin Translocation Induced by the P2Y Receptor Subtypes—To test for receptor-induced β-arrestin translocation, we co-transfected each individual P2Y receptor and β-arrestin-2-YFP in HEK-293 cells. Fig. 2*A* (*left panels*) shows the cytosolic distribution of β-arrestin-2-YFP prior to agonist stimulation. Upon stimulation with the appropriate agonist, the $P2Y_1$, $P2Y_2$, and $P2Y_4$ receptors caused rapid translocation of β-arrestin-2-YFP to the plasma membrane (Fig. 2*A*). In contrast, for the $P2Y_6$, $P2Y_{11}$, and $P2Y_{12}$ receptor, we did not observe any β-arrestin-2-YFP translocation (data not shown). To control for correct receptor expression, we used $P2Y_6$, $P2Y_{11}$, and $P2Y_{12}$ receptors C-terminally tagged with CFP. Although the $P2Y_6$, $P2Y_{11}$, and $P2Y_{12}$ receptors were clearly localized at the cell surface (Fig. 2*A*, *right panels*), they did not result in β-arrestin-2-YFP translocation to the plasma membrane (Fig. 2*A*, *center panels*). However, when GRK2 was co-transfected, there was some degree of β-arrestin-2-YFP translocation by the $P2Y_6$ and $P2Y_{11}$ but not the $P2Y_{12}$ receptor (Fig. 2*B*).

Similar experiments with β-arrestin-1-GFP showed modest translocation for the $P2Y_1$ receptor and strong translocation for

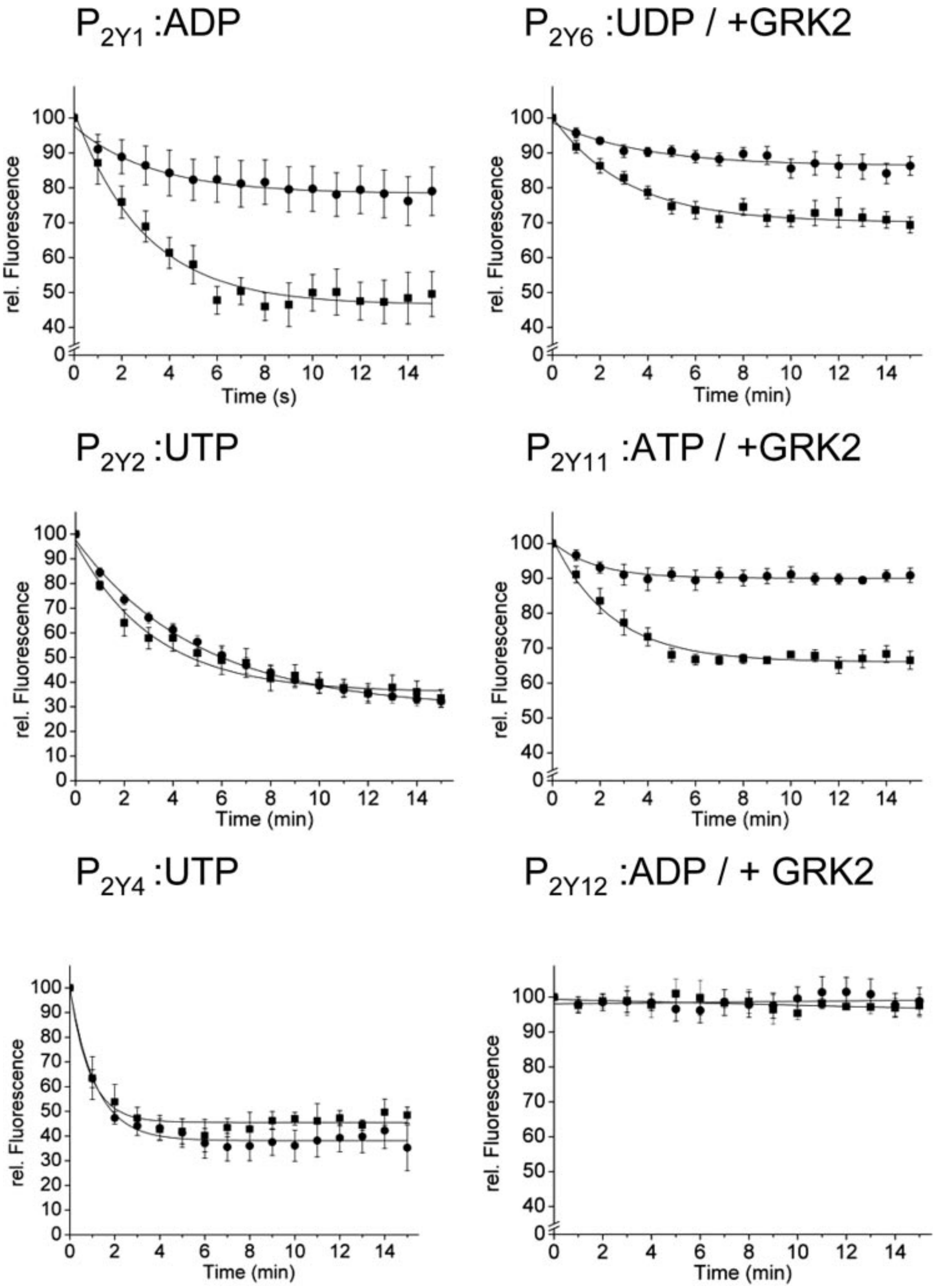

FIGURE 3. **Quantification of β-arrestin translocation induced by the P2Y$_{1,2,4,6,11,12}$ receptor.** Data from experiments as described in Fig. 2 and supplemental Fig. 2 were quantified and corrected for photobleaching as described under "Experimental Procedures." Cells were co-transfected with wild-type P2Y receptors, β-arrestin-1-GFP or β-arrestin-2-YFP, and GRK2 as indicated. *Circles* indicate β-arrestin-1-GFP translocation, and *squares* represent data for β-arrestin-2-YFP translocation. Data represent average data ± S.E. of 10–12 different cells from at least three different experiments.

the P2Y$_2$ and P2Y$_4$ receptors. In contrast, for the P2Y$_6$ and P2Y$_{11}$ receptors, only slight translocation was observed, and this required that the cells were co-transfected with GRK2, and no translocation was seen for the P2Y$_{12}$ receptor even when the cells were additionally co-transfected with GRK2 (supplemental Fig. 2).

Specificity of the observed β-arrestin translocation was again demonstrated by the use of specific antagonists. For example, MRS2179, a selective antagonist for the P2Y$_1$ receptor (9, 25), effectively and in a concentration-dependent manner blocked the ADP-mediated β-arrestin translocation by the P2Y$_1$ receptor (supplemental Fig. 3).

Quantification of β-Arrestin Translocation—A quantitative analysis of β-arrestin-1 and -2 translocation induced by the various P2Y receptors is presented in Fig. 3. According to the classification suggested by Oakley *et al.* (5), GPCRs are classified as class A when they induce stronger translocation for β-arrestin-2 than for β-arrestin-1, and as class B when β-arrestin-2 and -1 translocation are similar.

According to the results shown in Fig. 3, using the indicated nucleotide as the stimulus, the P2Y$_1$, P2Y$_6$, and P2Y$_{11}$ receptors can be classified as class A, whereas the P2Y$_2$ and P2Y$_4$ receptors would be classified as class B. The P2Y$_{12}$ receptor did not translocate either β-arrestin in our experiments and therefore cannot be classified.

Dynamin-dependent Receptor Internalization—Because receptor internalization has been described to often be dependent on clathrin and dynamin (26, 27), we decided to study the internalization of the P2Y receptor family with respect to dynamin dependence. YFP-tagged P2Y receptors were co-transfected with either rat dynamin 1a or a dominant negative dynamin mutant Dyn-K44A (21) and studied for ligand-induced receptor internalization. In control experiments, co-transfection with dynamin 1a did not have negative effects on receptor internalization but rather seemed to enhance internalization (data not shown). Co-expression of P2Y receptors, GRK-2 when needed, and Dyn-K44A blocked receptor internalization for all P2Y receptors except the P2Y$_2$ receptor (Fig. 4). Both ATP- and UTP-induced P2Y$_2$ receptor internalization was unaffected by co-expression of Dyn-K44A mutant (data not shown).

Differential Effects of the Two Endogenous P2Y$_2$ Receptor Ligands—The P2Y$_2$ receptor is a special receptor because it has two endogenous ligands of equal potency, ATP and UTP (19). This allowed an investigation of the question whether endogenous ligands might differ in their ability to induce specific translocation of β-arrestins.

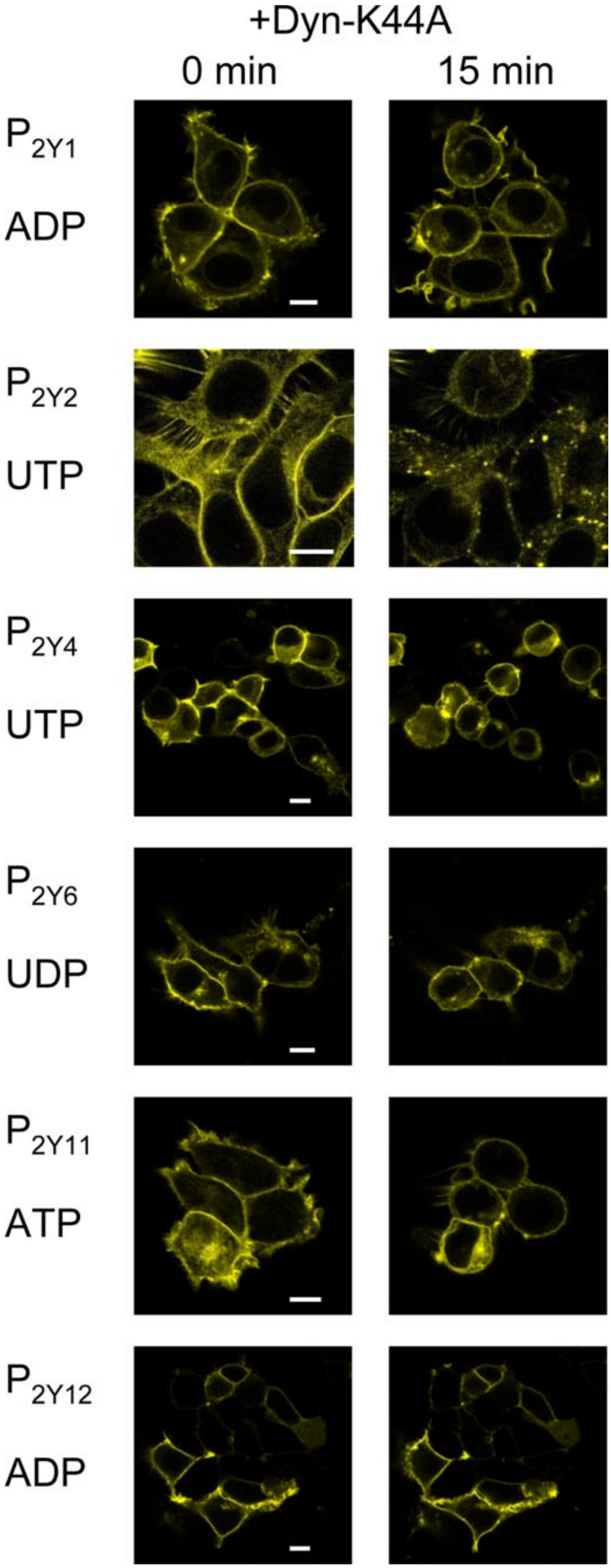

FIGURE 4. **Effect of dynamin-K44A on agonist-induced internalization of YFP-tagged $P2Y_{1,2,4,6,11,12}$ receptors in HEK-293 cells.** Cells were transfected with fluorescently tagged P2Y receptor constructs and dynamin-K44A mutant and studied for receptor internalization. The *left column* represents cells prior to stimulation with the indicated agonist. The *right column* shows the same cells 15 min after exposure to the indicated agonist. No punctate pattern was observed for the $P2Y_1$, $P2Y_4$, $P2Y_6$, $P2Y_{11}$, and $P2Y_{12}$ receptor tagged with YFP in the presence of dynamin K44A, whereas a punctate pattern still occurred for the $P2Y_2$ receptor. All agonist concentrations were 100 μM final. Data are representative examples of at least three individual experiments. *White scale bars* represent 10 μm.

Thus, analogous experiments were performed using 100 μM ATP, and quantitatively analyzed and compared with the results obtained with UTP (Fig. 5). ATP stimulation of the $P2Y_2$ receptor caused statistically significantly greater translocation of β-arrestin-1-GFP than of β-arrestin-2-YFP; in contrast, translocation was identical for the two β-arrestins when using UTP (Fig. 5*A*). When maximal translocation (15 min) was grouped according to the respective β-arrestin, UTP had significantly greater effects for β-arrestin-1-GFP ($p < 0.01$) but smaller effects for β-arrestin-2-YFP ($p < 0.05$; Fig. 5*B*).

To confirm this ligand/β-arrestin selectivity with another approach, we performed FRET measurements between β-arrestins labeled with the CFP-like cerulean protein and YFP-labeled receptors. This approach has been utilized and validated previously for the β_2-adrenergic receptor (16). It detects an increase in FRET between cerulean and YFP, when receptor and β-arrestin interact. A $P2Y_2$-YFP construct and a β-arrestin-1-cerulean construct were expressed in HEK-293 cells, and FRET was measured in individual cells, which were stimulated alternating between 100 μM ATP and UTP (Fig. 5*C*). It can be seen that in the case of β-arrestin-1, ATP caused a smaller increase in FRET than was observed upon stimulation of the same cell with UTP. The contrary was true for β-arrestin-2; here, ATP caused larger changes in FRET than UTP (Fig. 5*C*, *right panel*). Therefore, these data confirm our findings, shown in Fig. 5*B*, of preferential interactions of the $P2Y_2$ receptor with β-arrestin-1 and -2 induced by ATP and UTP, respectively.

To analyze the potential consequences of such ligand-dependent β-arrestin interaction, we studied receptor-mediated ERK phosphorylation, a pathway that is known to be partially β-arrestin-mediated (6). Because no selective radioligand for the $P2Y_2$ receptor is currently available to confirm receptor expression, we decided to generate a stable cell line using the $P2Y_2$-YFP receptor. Cells stably expressing the receptor construct were prepared for the experiments as described above and stimulated with ATP and UTP and analyzed for ligand-dependent ERK phosphorylation. Control experiments using nontransfected HEK-293 cells showed no ATP- or UTP-induced ERK-phosphorylation (data not shown). As shown in Fig. 5*D*, cells expressing the $P2Y_2$ receptor stimulated with ATP or UTP showed clear ERK phosphorylation. ATP and UTP exhibited a different time profile for receptor-mediated ERK phosphorylation. Although UTP exhibited a transient p-ERK signal, with a peak at 10 min, ATP showed prolonged ERK phosphorylation (Fig. 5*D*).

DISCUSSION

Our study shows that the receptor internalization and β-arrestin translocation profiles of the various P2Y receptor subtypes are markedly different. All of these receptors internalized

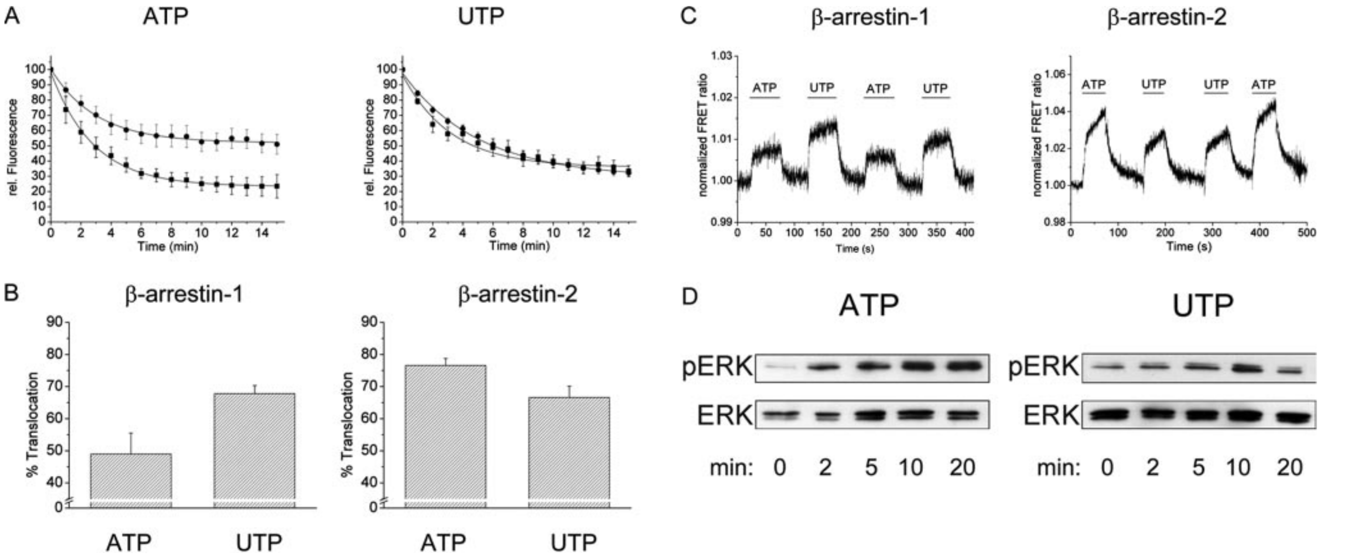

FIGURE 5. **Differential effects of the two endogenous P2Y$_2$ receptor ligands.** *A,* quantification of *β*-arrestin translocation after ATP (*left*) or UTP exposure (*right*). Data were quantified and corrected for photobleaching as described under "Experimental Procedures." *Circles* represent translocation of *β*-arrestin-1-GFP, and *squares* represent translocation of *β*-arrestin-2-YFP. Data are average data ± S.E. from 10 to 12 cells of at least three different experiments. *B,* data from 15-min time points after agonist-induced arrestin translocation of panel (Fig. 4, *left* and *right*) were recalculated as % translocation (100% minus remaining cytosolic fluorescence) and presented as sorted for *β*-arrestin-1 or -2 rather than agonist. UTP exhibited stronger translocation for *β*-arrestin-1 than ATP ($p < 0.01$), whereas ATP exhibited stronger translocation for *β*-arrestin-2 than UTP ($p < 0.05$). *C, left,* detection of interactions between P2Y$_2$-YFP and *β*-arrestin-1-Cerulean by FRET. Normalized FRET ratios (F_{YFP}/F_{CFP}) of single cells co-transfected with P2Y$_2$-YFP and *β*-arrestin-1-Cerulean (*left panel*) or P2Y$_2$-YFP and *β*-arrestin-2-CFP (*right panel*) are shown. The cells were constantly superfused with buffer or buffer supplemented with ATP or UTP as described. Sample traces are shown that are representative for seven cells in three different experiments. *D, left,* time dependence of ATP (100 μM)-stimulated ERK phosphorylation in HEK-293 cells stably expressing human P2Y$_2$-YFP receptor; *right*, time dependence of UTP (100 μM)-stimulated ERK phosphorylation in HEK-293 cells stably expressing human P2Y$_2$ receptor. The data shown are representative for six individual experiments with ATP and UTP done in parallel.

in an agonist-dependent manner, but some of them required co-expression with GRK2. All P2Y receptors also showed some degree of interaction with *β*-arrestins, again in several cases only after co-transfection of GRK2. The most interesting finding is the observations that different endogenous agonists for the P2Y$_2$ receptor have distinct effects on the *β*-arrestin translocation and interaction profile.

All six P2Y receptor subtypes investigated in this study were found to internalize upon agonist stimulation. Although the P2Y$_1$, P2Y$_2$, and P2Y$_4$ receptors internalized in normal HEK-293 cells (Fig. 1*A*), the P2Y$_6$, P2Y$_{11}$, and P2Y$_{12}$ receptors required co-transfection of GRK2 for internalization (Fig. 1*B*). Agonist-dependent internalization has already been described for P2Y$_1$ (12, 20, 29, 30), P2Y$_2$ (29, 31, 32), and P2Y$_4$ (33). In contrast, the P2Y$_6$ receptor has been described as slowly desensitizing (34) and resistant to internalization (33), whereas the P2Y$_{11}$ receptors has been shown to internalize only as heterodimer with the P2Y$_1$ receptor, but not alone (13). Conflicting data describe internalization of P2Y$_{12}$ receptors as either very modest (20) or quite pronounced (12, 35). The latter data may be explained by our observation that effective internalization of these receptors required co-expression of GRK2 (Fig. 1*B*).

Divergent kinases have been implicated in the internalization process, including calmodulin-dependent kinase II (30), PKC*α*- and *δ*-isoforms (11), and GRK2 and -6, whereas other reports suggest that GRK2, GRK6 PKC, and calmodulin-dependent kinase II were *not* involved (12, 35–38).

Very little was known about the involvement of *β*-arrestins in P2Y receptor internalization. Stimulation of P2Y$_{12}$ receptors was recently reported to recruit *β*-arrestin-1 and -2 into lipid rafts (39) and to translocate *β*-arrestin-1-GFP to the cell surface (12). In contrast, no *β*-arrestin-1-GFP translocation was observed for the P2Y$_1$ (12).

Our data contrast with these findings. As shown in Fig. 3 and supplemental Figs. 2 and 3, the P2Y$_1$ receptor *did* translocate *β*-arrestin-1-GFP in an agonist-dependent and specific manner, but to a much lower extent than *β*-arrestin-2-YFP; this classifies the P2Y$_1$ receptor as a class A receptor.

For the P2Y$_{12}$ receptor, we failed to observe *β*-arrestin translocation by confocal microscopy (Fig. 2, *A* and *B*, and supplemental Fig. 2), but we were able to detect a direct, agonist-dependent interaction of the P2Y$_{12}$-YFP receptor and *β*-arrestin-2-CFP by FRET (supplemental Fig. 5). This suggests that FRET is a more sensitive method to discover such receptor/*β*-arrestin interactions.

For all other P2Y receptor subtypes included in this study, *β*-arrestin translocation was demonstrated by means of confocal microscopy, permitting a classification as either class A or class B. These experiments revealed that the P2Y$_1$, P2Y$_6$, and P2Y$_{11}$ receptors can be classified as class A receptors, whereas the P2Y$_4$ receptor can be classified as a class B receptor.

To further investigate the mechanism of receptor internalization, we tested the involved pathway by co-expressing a dominant negative dynamin variant Dyn-K44A. This mutant has been described to block the dynamin-dependent internalization pathway (21). As shown in Fig. 4, we observed dynamin-dependent receptor internalization in case of the P2Y$_{1,4,6,11,12}$ receptor, whereas the P2Y$_2$ receptor internalization was found to be independent of dynamin. The data for P2Y$_1$ and P2Y$_{12}$ are consistent with previous data (12), and the P2Y$_2$ receptor would employ an alternative dynamin-independent internalization pathway (27). Strikingly, the rat P2Y$_2$ receptor has been described to co-localize with clathrin (30), which may imply that the rat and human receptor may be differently regulated.

The most interesting finding of our study is the differential β-arrestin translocation pattern that was observed for the P2Y$_2$ receptor. As shown in Fig. 5, UTP translocated β-arrestin-1 and -2 to the same extent, which would classify the P2Y$_2$ receptor as class B. In contrast, ATP is much weaker in translocating β-arrestin-1 than β-arrestin-2, thus classifying the receptor as class A. The same differential pattern was found when we investigated the direct interaction between receptors and β-arrestins with FRET (Fig. 5*C*). Interestingly, a ligand-mediated differential signaling behavior was observed when we investigated ERK phosphorylation as the major signaling pathway, which is triggered by β-arrestins (6). The ATP-induced ERK phosphorylation was prolonged compared with the transient stimulation induced by UTP (Fig. 5*D*), and it would nicely match the time pattern that has been described for β-arrestin-mediated ERK phosphorylation (6). This ligand-dependent regulation of ERK phosphorylation mediated by the human P2Y$_2$ receptor not been described previously. Therefore, we conclude that we have found the first differential agonist behavior of ATP and UTP at the P2Y$_2$ receptor.

Classical receptor theory is based on the simple concept that receptors switch between an "off" and an "on" state and that agonists induce the on state. However, recent evidence along several lines suggests that this concept is insufficient and that there may be multiple agonist-induced "active" conformations (40–42). This hypothesis is based on several lines of evidence, including differential agonist-specific changes in fluorescently labeled $β_2$-adrenergic receptors (43), differential switching kinetics of partial *versus* full agonists (44), and agonist-selective signaling of receptors to G-proteins *versus* β-arrestins (28, 45, 46). Our data are the first to suggest that such selective signaling can occur with different endogenous agonists for a single receptor. They further show that agonist selectivity may not only be found in G-protein *versus* β-arrestin signaling but also in β-arrestin-1 *versus* -2 interaction, leading to classification as class A *versus* class B.

In summary, all six P2Y receptors investigated in this study internalized upon agonist stimulation. Although the P2Y$_1$, P2Y$_2$, and P2Y$_4$ receptors readily internalized in HEK-293 cells, the P2Y$_6$, P2Y$_{11}$, and P2Y$_{12}$ receptors required co-expression of GRK2 for internalization. All receptors interacted with β-arrestin-2, and this interaction showed the same GRK2 dependence as receptor internalization. According to their arrestin interaction profile, the P2Y$_1$, P2Y$_6$, and P2Y$_{11}$ receptors were classified as class A receptors, whereas the P2Y$_4$ receptor was classified as a class B receptor. The P2Y$_{12}$ receptor could not be classified, but interaction with β-arrestin-2 was demonstrated by FRET. Most importantly, the P2Y$_2$ receptor exhibited an agonist-dependent β-arrestin translocation profile. Upon stimulation with ATP, this would be classified as class A, whereas stimulation with UTP would classify the receptor as class B. This suggests that the two agonists induced different active conformations of the P2Y$_2$ receptor, which behaved differently with respect to β-arrestin recruitment and ERK phosphorylation. Such differences in response to two different endogenous agonists represent a new example of fine-tuning in receptor signaling.

Acknowledgment—Constructs for rat dynamin-1a and the dynK44A mutant were kindly provided by Marc Caron (Duke University, Durham, NC).

REFERENCES

1. Gilman, A. G. (1987) *Annu. Rev. Biochem.* **56,** 615–6491
2. Kohout, T. A., and Lefkowitz, R. J. (2003) *Mol. Pharmacol.* **63,** 9–18
3. Lohse, M. J., Benovic, J. L., Codina, J., Caron, M. G., and Lefkowitz, R. J. (1990) *Science* **248,** 1547–1550
4. Shenoy, S. K., and Lefkowitz, R. J. (2003) *Biochem. J.* **375,** 503–515
5. Oakley, R. H., Laporte, S. A., Holt, J. A., Caron, M. G., and Barak, L. S. (2000) *J. Biol. Chem.* **275,** 17201–17210
6. Lefkowitz, R. J., and Shenoy, S. K. (2005) *Science* **308,** 512–517
7. Burnstock, G. (2006) *Pharmacol. Rev.* **58,** 58–86
8. Abbracchio, M. P., Burnstock, G., Boeynaems, J. M., Barnard, E. A., Boyer, J. L., Kennedy, C., Knight, G. E., Fumagalli, M., Gachet, C., Jacobson, K. A., and Weisman, G. A. (2006) *Pharmacol. Rev.* **58,** 281–341
9. von Kugelgen, I. (2006) *Pharmacol. Ther.* **110,** 415–432
10. Burnstock, G., and Knight, G. E. (2004) *Int. Rev. Cytol.* **240,** 31–304
11. Mundell, S. J., Jones, M. L., Hardy, A. R., Barton, J. F., Beaucourt, S. M., Conley, P. B., and Poole, A. W. (2006) *Mol. Pharmacol.* **70,** 1132–1142
12. Mundell, S. J., Luo, J., Benovic, J. L., Conley, P. B., and Poole, A. W. (2006) *Traffic* **7,** 1420–1431
13. Ecke, D., Hanck, T., Tulapurkar, M. E., Schafer, R., Kassack, M., Stricker, R., and Reiser, G. (2008) *Biochem. J.* **409,** 107–116
14. Hoffmann, C., Soltysiak, K., West, P. L., and Jacobson, K. A. (2004) *Biochem. Pharmacol.* **68,** 2075–2086
15. Ho, S. N., Hunt, H. D., Horton, R. M., Pullen, J. K., and Pease, L. R. (1989) *Gene* (*Amst.*) **77,** 51–59
16. Krasel, C., Bunemann, M., Lorenz, K., and Lohse, M. J. (2005) *J. Biol. Chem.* **280,** 9528–9535
17. Rizzo, M. A., Springer, G. H., Granada, B., and Piston, D. W. (2004) *Nat. Biotechnol.* **22,** 445–449
18. Hoffmann, C., Moro, S., Nicholas, R. A., Harden, T. K., and Jacobson, K. A. (1999) *J. Biol. Chem.* **274,** 14639–14647
19. Nicholas, R. A., Watt, W. C., Lazarowski, E. R., Li, Q., and Harden, K. (1996) *Mol. Pharmacol.* **50,** 224–229
20. Baurand, A., Eckly, A., Hechler, B., Kauffenstein, G., Galzi, J. L., Cazenave, J. P., Leon, C., and Gachet, C. (2005) *Mol. Pharmacol.* **67,** 721–733
21. Zhang, J., Barak, L. S., Winkler, K. E., Caron, M. G., and Ferguson, S. S. (1997) *J. Biol. Chem.* **272,** 27005–27014
22. Fischer, W., Franke, H., Groger-Arndt, H., and Illes, P. (2005) *Naunyn-Schmiedeberg's Arch. Pharmacol.* **371,** 466–472
23. Kennedy, C., Qi, A. D., Herold, C. L., Harden, T. K., and Nicholas, R. A. (2000) *Mol. Pharmacol.* **57,** 926–931
24. Herold, C. L., Qi, A. D., Harden, T. K., and Nicholas, R. A. (2004) *J. Biol. Chem.* **279,** 11456–11464
25. Camaioni, E., Boyer, J. L., Mohanram, A., Harden, T. K., and Jacobson, K. A. (1998) *J. Med. Chem.* **41,** 183–190
26. Ferguson, S. S. (2001) *Pharmacol. Rev.* **53,** 1–24
27. Mayor, S., and Pagano, R. E. (2007) *Nat. Rev. Mol. Cell Biol.* **8,** 603–612
28. Drake, M. T., Violin, J. D., Whalen, E. J., Wisler, J. W., Shenoy, S. K., and Lefkowitz, R. J. (2007) *J. Biol. Chem.* **283,** 5669–5676
29. Tulapurkar, M. E., Laubinger, W., Nahum, V., Fischer, B., and Reiser, G. (2004) *Br. J. Pharmacol.* **142,** 869–878
30. Tulapurkar, M. E., Zundorf, G., and Reiser, G. (2006) *J. Neurochem.* **96,** 624–634
31. Sromek, S. M., and Harden, T. K. (1998) *Mol. Pharmacol.* **54,** 485–494
32. Garrad, R. C., Otero, M. A., Erb, L., Theiss, P. M., Clarke, L. L., Gonzalez, F. A., Turner, J. T., and Weisman, G. A. (1998) *J. Biol. Chem.* **273,** 29437–29444
33. Brinson, A. E., and Harden, T. K. (2001) *J. Biol. Chem.* **276,** 11939–11948
34. Robaye, B., Boeynaems, J. M., and Communi, D. (1997) *Eur. J. Pharmacol.*

329, 231–236

35. Hardy, A. R., Conley, P. B., Luo, J., Benovic, J. L., Poole, A. W., and Mundell, S. J. (2005) *Blood* **105,** 3552–3560
36. Otero, M., Garrad, R. C., Velazquez, B., Hernandez-Perez, M. G., Camden, J. M., Erb, L., Clarke, L. L., Turner, J. T., Weisman, G. A., and Gonzalez, F. A. (2000) *Mol. Cell. Biochem.* **205,** 115–123
37. Flores, R. V., Hernandez-Perez, M. G., Aquino, E., Garrad, R. C., Weisman, G. A., and Gonzalez, F. A. (2005) *Mol. Cell. Biochem.* **280,** 35–45
38. Del Rey, A., Renigunta, V., Dalpke, A. H., Leipziger, J., Matos, J. E., Robaye, B., Zuzarte, M., Kavelaars, A., and Hanley, P. J. (2006) *J. Biol. Chem.* **281,** 35147–35155
39. Savi, P., Zachayus, J. L., Delesque-Touchard, N., Labouret, C., Herve, C., Uzabiaga, M. F., Pereillo, J. M., Culouscou, J. M., Bono, F., Ferrara, P., and Herbert, J. M. (2006) *Proc. Natl. Acad. Sci. U. S. A.* **103,** 11069–11074
40. Kenakin, T. (2007) *Mol. Pharmacol.* **72,** 1393–1401
41. Galandrin, S., Oligny-Longpre, G., and Bouvier, M. (2007) *Trends Pharmacol. Sci.* **28,** 423–430
42. Hoffmann, C., Zurn, A., Bunemann, M., and Lohse, M. J. (2008) *Br. J. Pharmacol.* **153,** Suppl. 1, 358–366
43. Kobilka, B. K., and Deupi, X. (2007) *Trends Pharmacol. Sci.* **28,** 397–406
44. Nikolaev, V. O., Hoffmann, C., Bunemann, M., Lohse, M. J., and Vilardaga, J. P. (2006) *J. Biol. Chem.* **281,** 24506–24511
45. Wei, H., Ahn, S., Shenoy, S. K., Karnik, S. S., Hunyady, L., Luttrell, L. M., and Lefkowitz, R. J. (2003) *Proc. Natl. Acad. Sci. U. S. A.* **100,** 10782–10787
46. Schonbrunn, A. (2008) *Mol. Cell. Endocrinol.* **286,** 35–39